Supplementary Material for
A Microfluidic Device for Dry Sample Preservation in Remote Settings

Stefano Begolo,[†] Feng Shen,[‡] and Rustem F. Ismagilov[†]*

[†] *Division of Chemistry and Chemical Engineering, California Institute of Technology, 1200 East California Boulevard, Pasadena, California 91125, United States*

[‡] *SlipChip, LLC, 129 N. Hill Ave., Pasadena, CA 91106*

*Corresponding author: rustem.admin@caltech.edu

SUPPORTING MOVIES

All videos were filmed with an early prototype of the device that relied on screws, rather than the improved press-fit system (Fig. S5), for clamping the device.

Video keywords: diagnostics, sample transportation, biosurveillance, biological archiving, sample preservation, microfluidics, remote analysis

Video S1: Sample preservation device filling. This video illustrates device filling, which can be performed by an untrained user. Once the user slips the device, it can be shipped to a laboratory for analysis. From "A Microfluidic Device for Dry Sample Preservation in Remote Settings," by Stefano Begolo, Feng Shen, and Rustem F. Ismagilov.

Video S2: Dynamics of drying on a sample preservation device. This video shows the process of sample drying within the device. Movie plays 60x faster than real-time. From "A Microfluidic Device for Dry Sample Preservation in Remote Settings," by Stefano Begolo, Feng Shen, and Rustem F. Ismagilov.

Video S3: Sample re-collection from a sample preservation device. This movie details the steps for rehydrating and recovering dried samples (rehydration section plays 8x faster than real-time). Rehydration and recollection are shown only for one well, demonstrating the capability for partial recovery. From "A Microfluidic Device for Dry Sample Preservation in Remote Settings," by Stefano Begolo, Feng Shen, and Rustem F. Ismagilov.

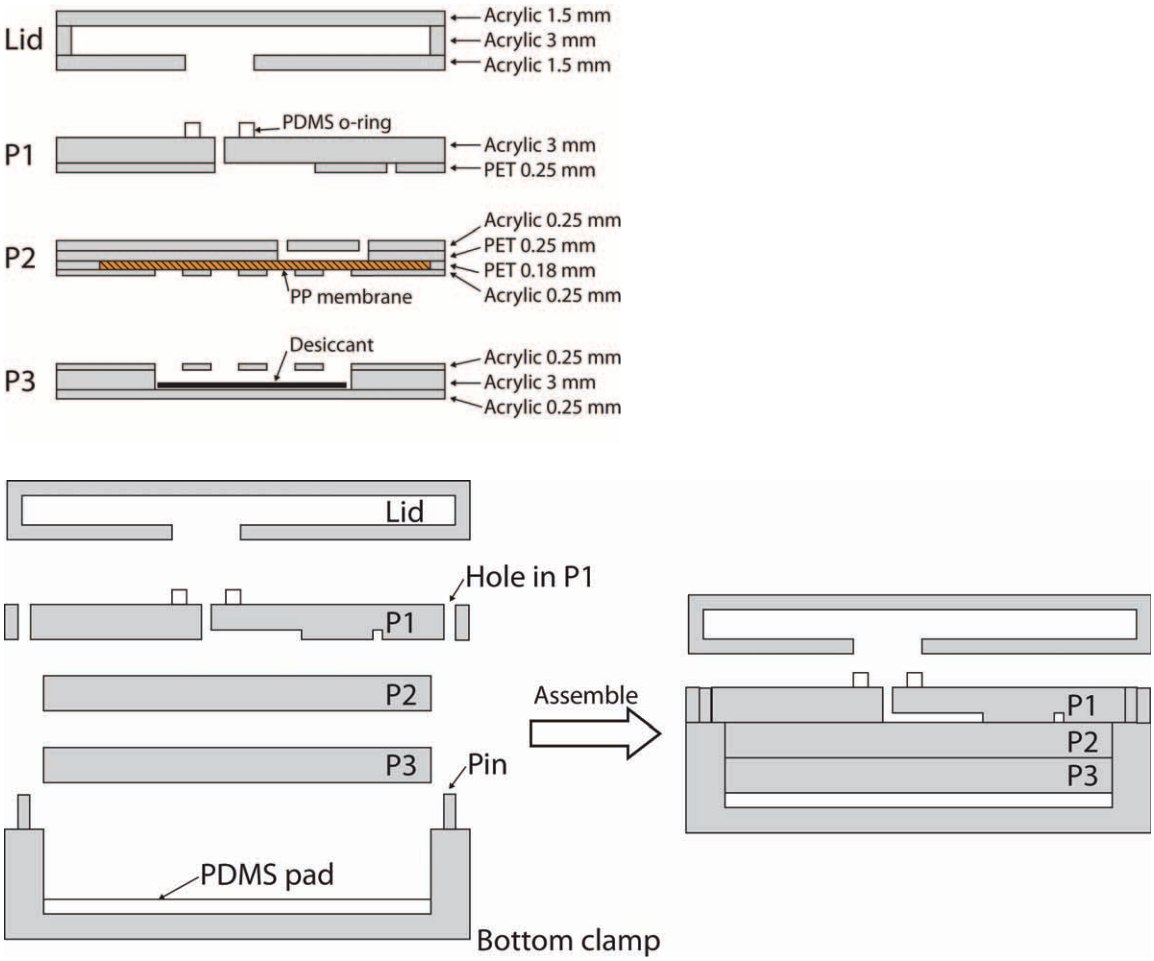

Fig. S1 A schematic drawing of the materials composing each part of the device (top) and the assembly strategy using a pin and hole approach to clamp the device (bottom).

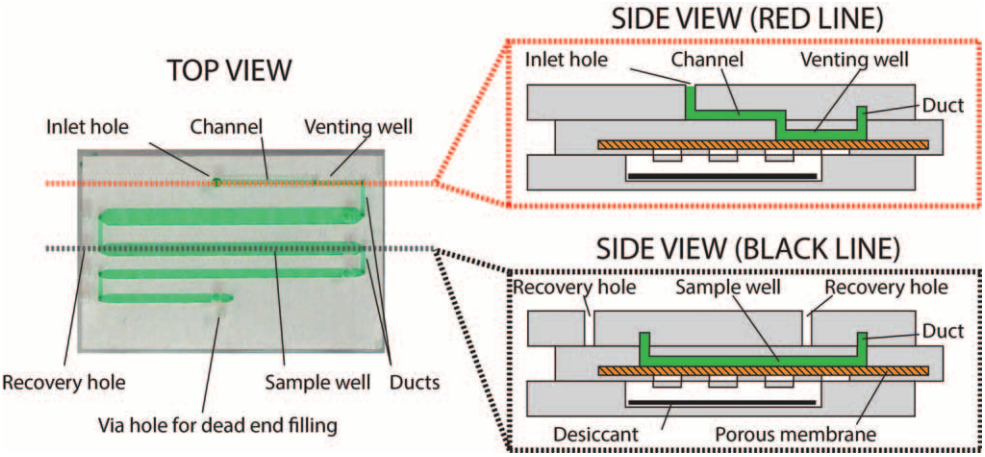

Fig. S2 A top-view photo of the device (left) with side-view drawings showing device structure (right).

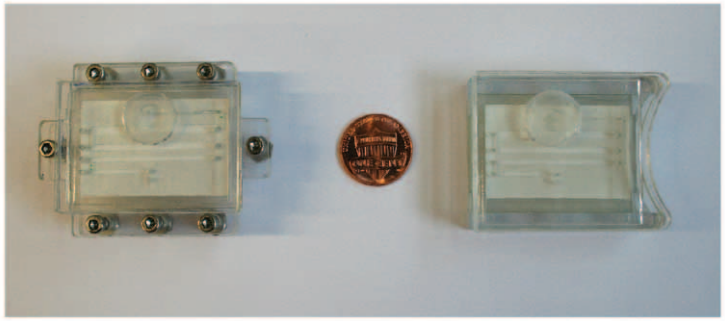

Fig. S3 A photograph of the prototype devices used for this work. Left: the first iteration of development, in which clamping was achieved using metal screws. Right: an improved iteration of the device, which uses self-clamping parts (pins are press-fit into holes to create tension and hold the device together). Although these devices are prototypes, the designs were made in consultation with manufacturers to ensure compatibility with mass production.

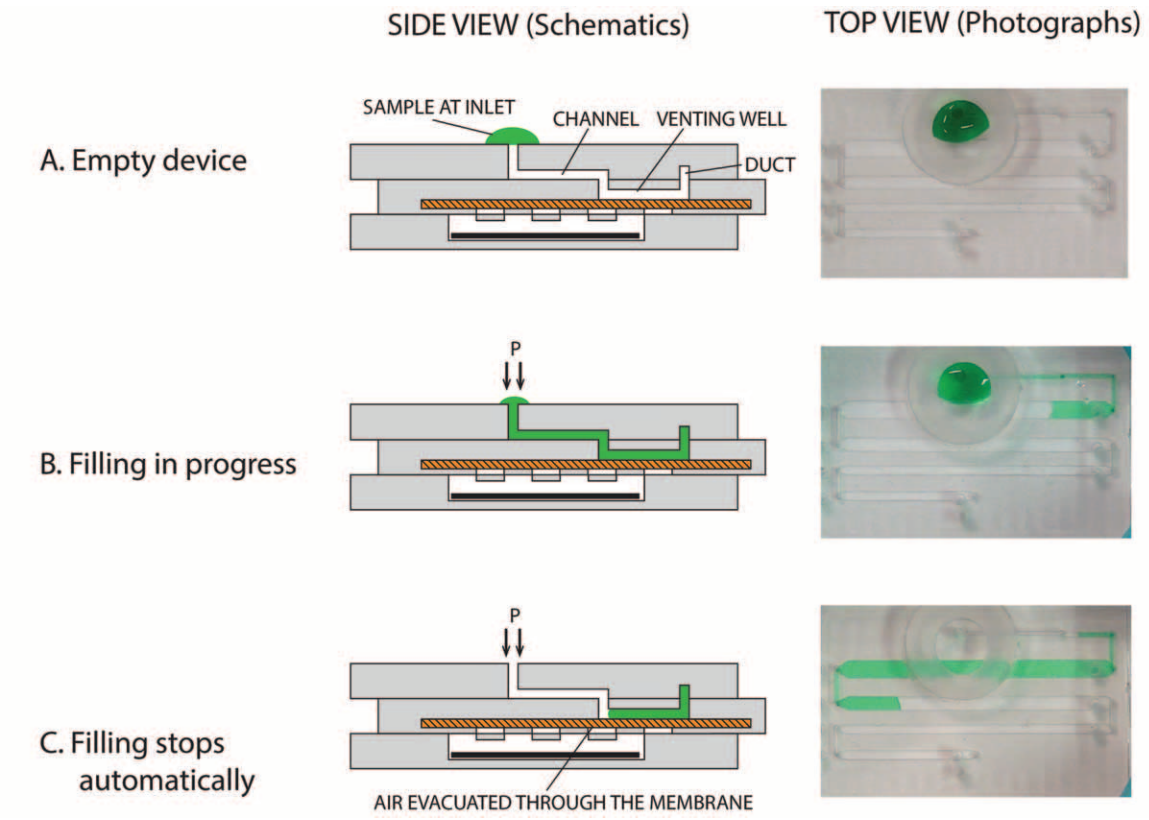

Fig. S4 Schematic drawings (left) and photographs (right) showing the "venting well" mechanism. An extra well (venting well) is added near the device inlet. When loading a sample, the air originally present in the wells and channels is evacuated through the membrane to the external atmosphere. A similar approach is used to prevent the accidental injection of air into the device: if air is injected (e.g., due to the presence of a bubble or due to the fact that all of the liquid sample has been already injected), this air is evacuated through the porous membrane and does not reach the storage wells. This stops the filling and prevents any issue with volume quantification using the storage device.

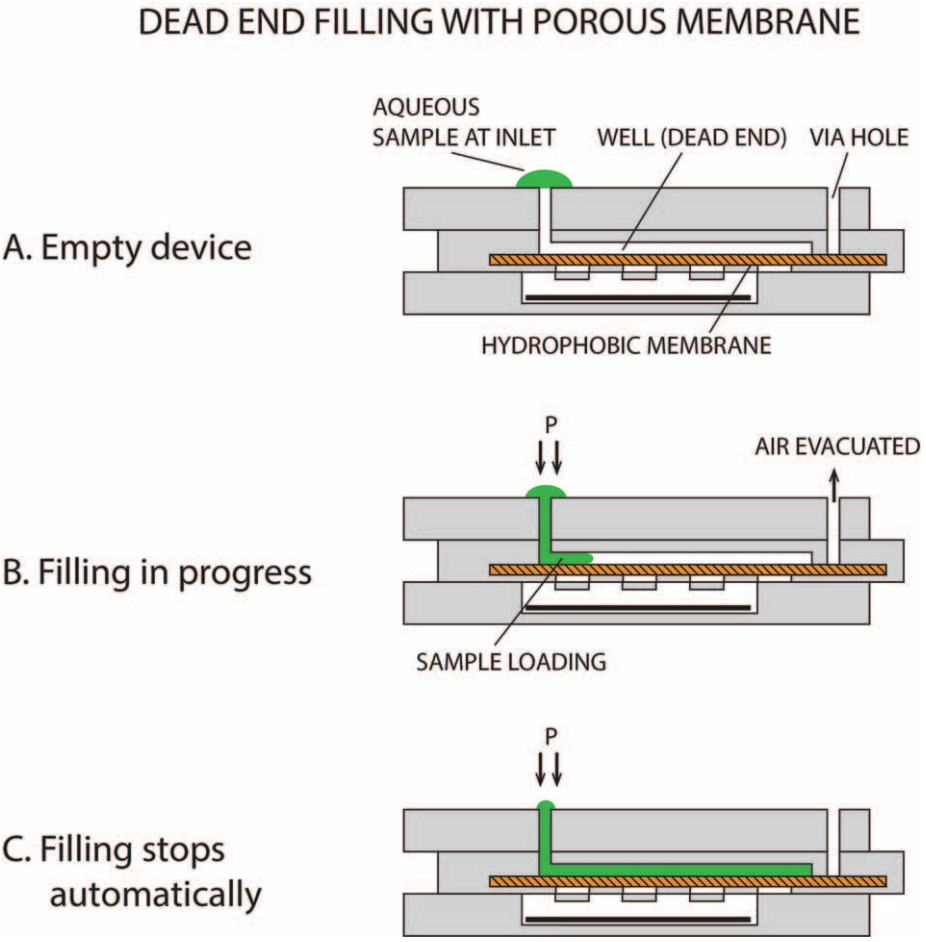

Fig. S5 Schematic drawings showing the "dead-end filling" mechanism using a porous membrane. The well to be filled has only one inlet and an extra "via hole" was added in the proximity of the end of the channel. When the sample is loaded into the device, the air originally present in the well is pushed through the membrane and evacuated through the via hole. The membrane is hydrophobic and has 0.45 μm pores, so it acts as a selective barrier. Air can pass easily through the membrane, while aqueous solutions cannot penetrate the pores at the pressures used for loading, due to capillary action. When the device wells are completely filled with the aqueous sample, loading stops automatically.

Table S1. A table summarizing the loading speeds and properties of various fluids that were loaded into the device.

Aqueous Phase	Aqueous Viscosity (mPa s)	Continuous phase	Continuous Phase Viscosity (mPa s)	Surface Tension (mN/m)	Pressure (mBar)	Loading volume (µL)	Total time	Average flow rate (µL/s)
Water	1	Air	~0	~50	76	50uL	4s	12.5
Water	1	Air	~0	~50	76	50 uL	5s	10
85% Glycerol 15% Water	110	Air	~0	~50	76	50uL	35s	1.4
85% Glycerol 15% Water	110	Air	~0	~50	76	50 uL	2min	0.4
Water + 0.4mM BSA	1	Air	~0	~7	76	50 uL	18 s	2.8

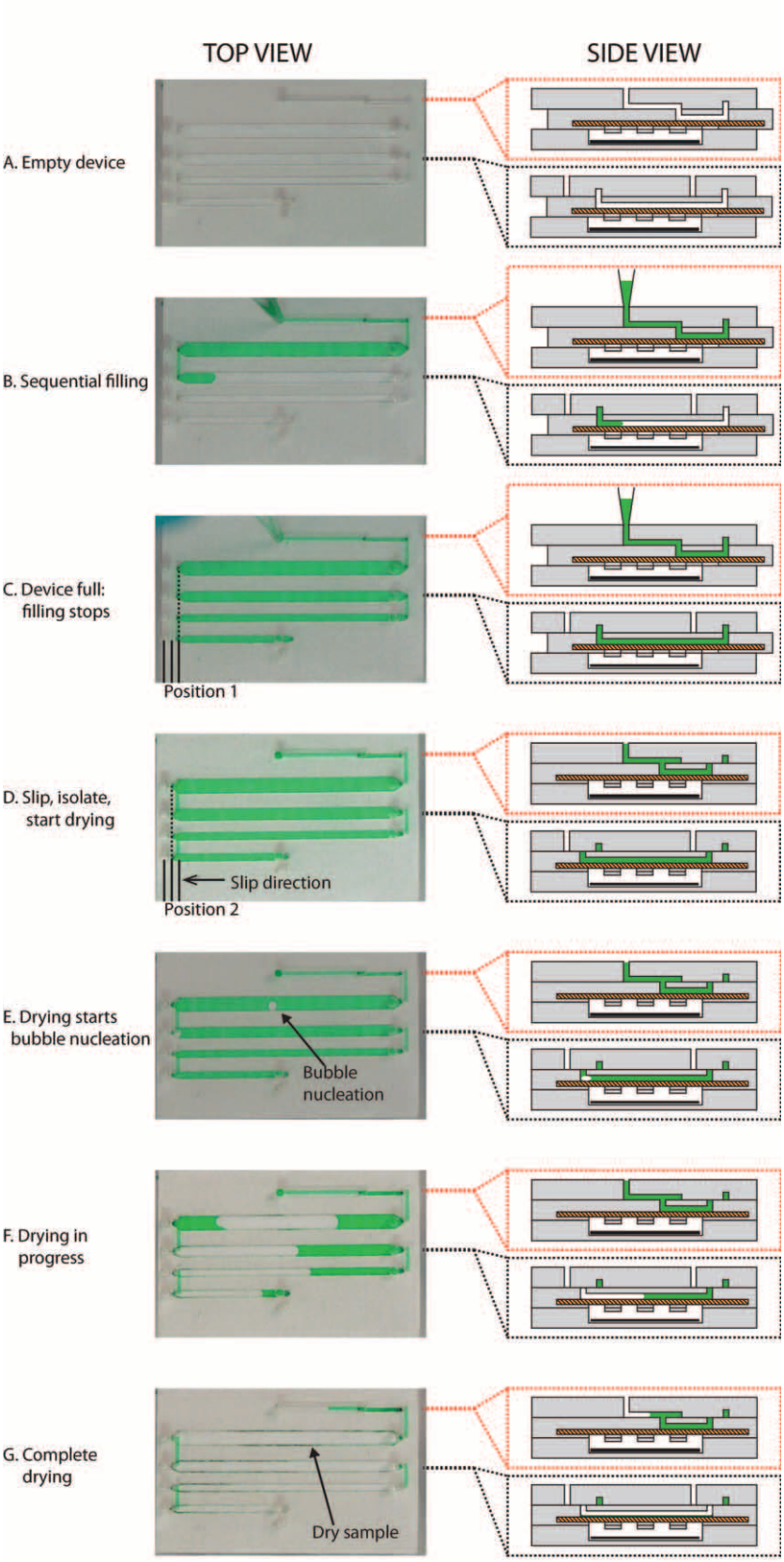

Fig. S6 Photographs (left) and drawings (right) showing steps for loading the device and drying samples.

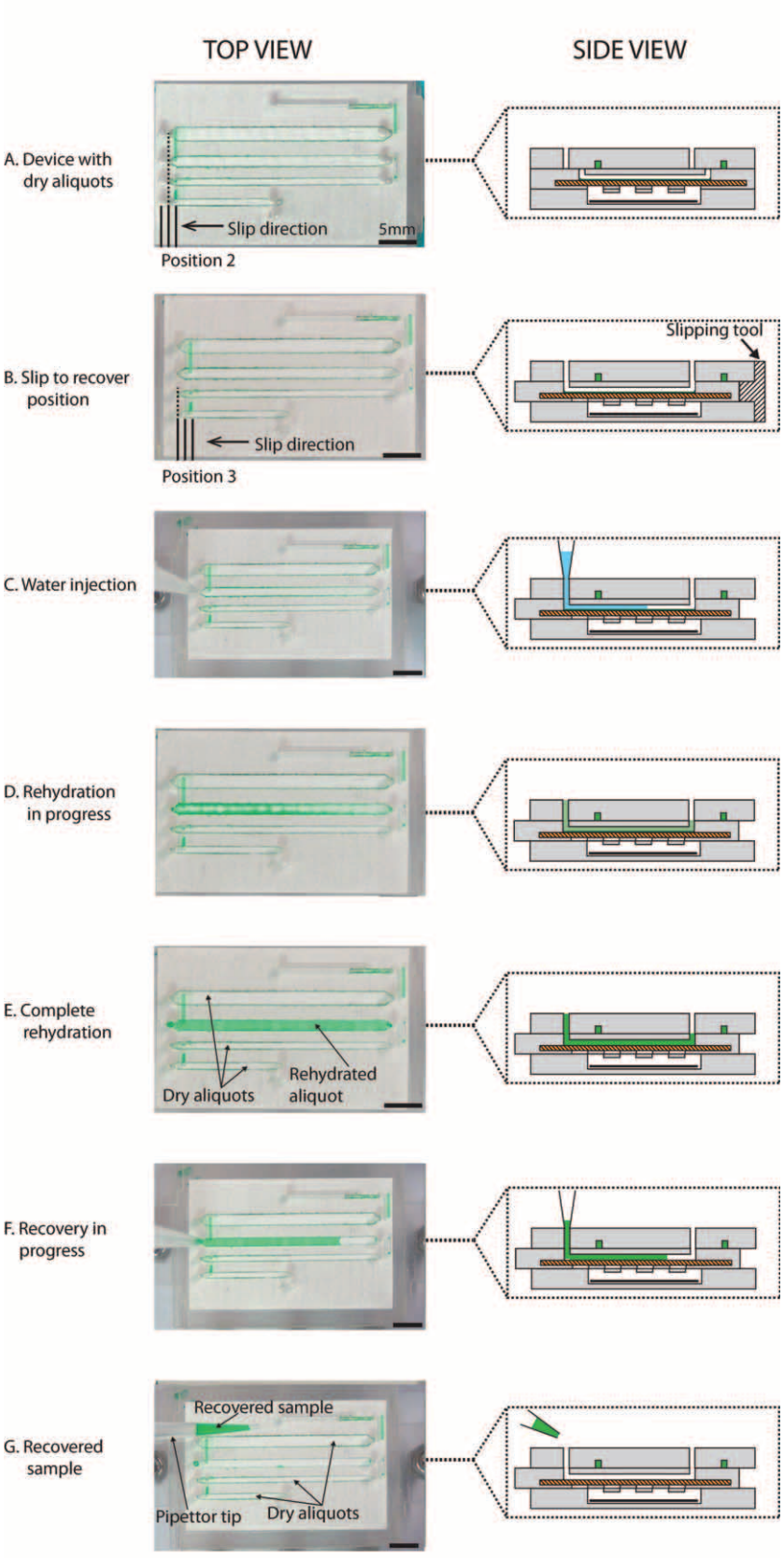

Fig. S7 Photographs (left) and drawings (right) showing each step of sample recovery from the device.

Table S2. Statistical analysis for Alexa Fluor 488 experiments.

Experimental results:

Sample	Fluorescence 30 μM (A.U.)		Fluorescence 60 μM (A.U.)		Fluorescence 120 μM (A.U.)
Control 1	623		1203		2946
Control 2	626		1224		2850
Control 3	625		1235		2789
Average:	**625**		**1220**		**2862**
St. Dev.	**1**		**16**		**78**
95% Confidence Interval +/-	**3**		**49**		**237**
Device 1	570		1256		2657
Device 2	586		1236		2681
Device 3	657		1312		2648
Device 4	611		1409		2606
Average:	**607**		**1304**		**2649**
St. Dev.	**38**		**78**		**31**
95% Confidence Interval	**114**		**234**		**94**
% of Recovery	**97%**		**106%**		**93%**

P-values (Student T test, 2 tails, unequal variances).

Comparison	Control	Device
30 μM vs 60 μM	2.38 E-04	4.88 E-05
60 μM vs 120 μM	4.88 E-04	6.41 E-06

Table S3. Statistical analysis for quantum dots experiments.

Experimental results:

Sample	Fluorescence 1x (A.U.)		Fluorescence 2x (A.U.)		Fluorescence 4x (A.U.)
Control 1	479		1039		1847
Control 2	481		990		1868
Control 3	461		994		1922
Average:	**474**		**1008**		**1879**
St. Dev.	**11**		**27**		**39**
95% Confidence Interval +/-	**33**		**81**		**116**
Device 1	459		965		1960
Device 2	457		962		1955
Device 3	440		922		1867
Device 4	428				1997
Average:	**446**		**950**		**1945**
St. Dev.	**15**		**24**		**55**
95% Confidence Interval	**44**		**72**		**165**
% of Recovery	**94%**		**94%**		**104%**

P-values (Student T test, 2 tails, unequal variances).

Comparison	Control	Device
1x vs 2x	1.7 E-04	5.1 E-05
2x vs 4x	1.5 E-05	2.7 E-06

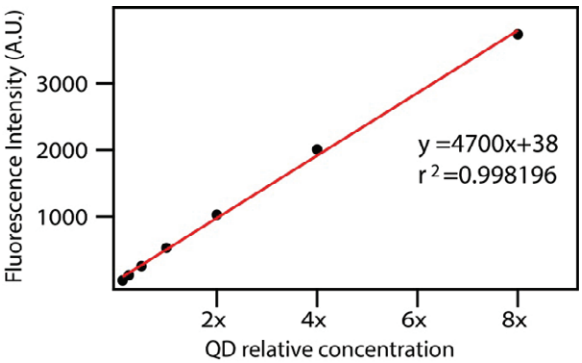

Fig. S8 Calibration curves for quantum dot solutions at different concentrations.

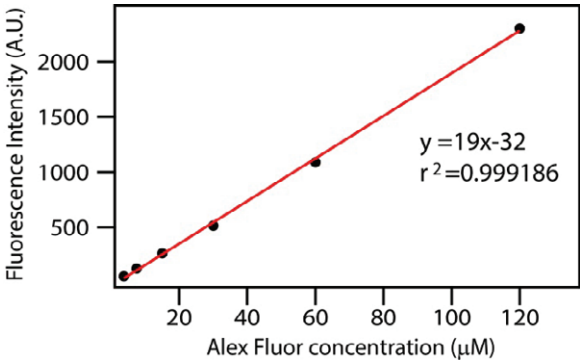

Fig. S9 Calibration curves for Alexa Fluor 488 solutions at different concentrations.

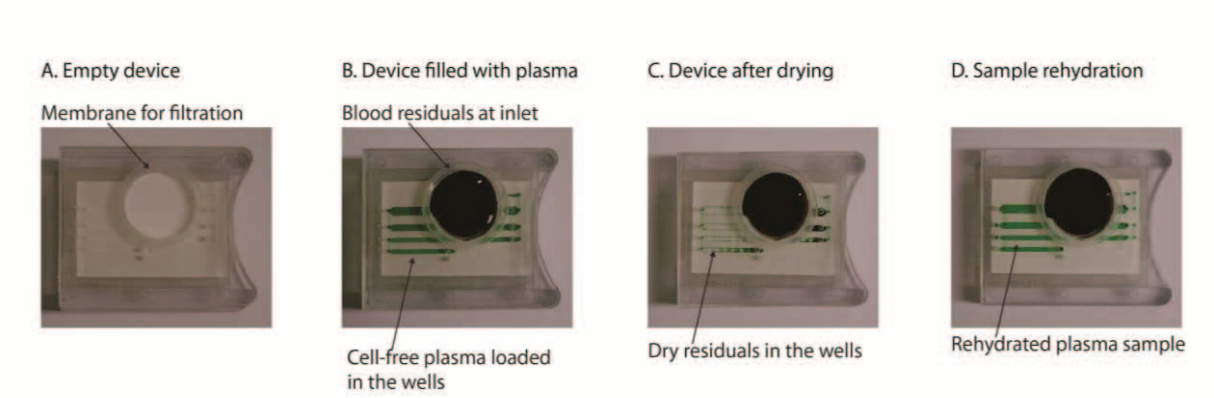

Fig. S10 Photographs of the device during plasma separation. Cell-free plasma contains a green food dye that aids visualization.

Table S4. Statistical analysis for HIV-1 recovery from plasma samples

Statistical analysis for HIV-1 recovery from plasma samples

Concentration	5.00E+05 copies / mL			4.00E+06 copies / mL	
	Centrifuge	Device		Centrifuge	Device
	35.73	35.62		33.05	33.45
	35.99	35.56		33.01	33.33
	35.65	35.28		32.36	33.61
	35.54				
	36.63				
	35.27				
Average	35.80	35.49		32.81	33.46
St. Dev.	0.47	0.18		0.39	0.14
95% Confidence Interval	1.43	0.55		1.18	0.43
Cq Difference	-0.31			0.65	
% Recovery	123%			66%	
P-values	0.38			0.085	

P-values (Student T test, 2 tails, unequal variances)

	p-value between different concentrations
Centrifuge	0.00017
Device	0.00016

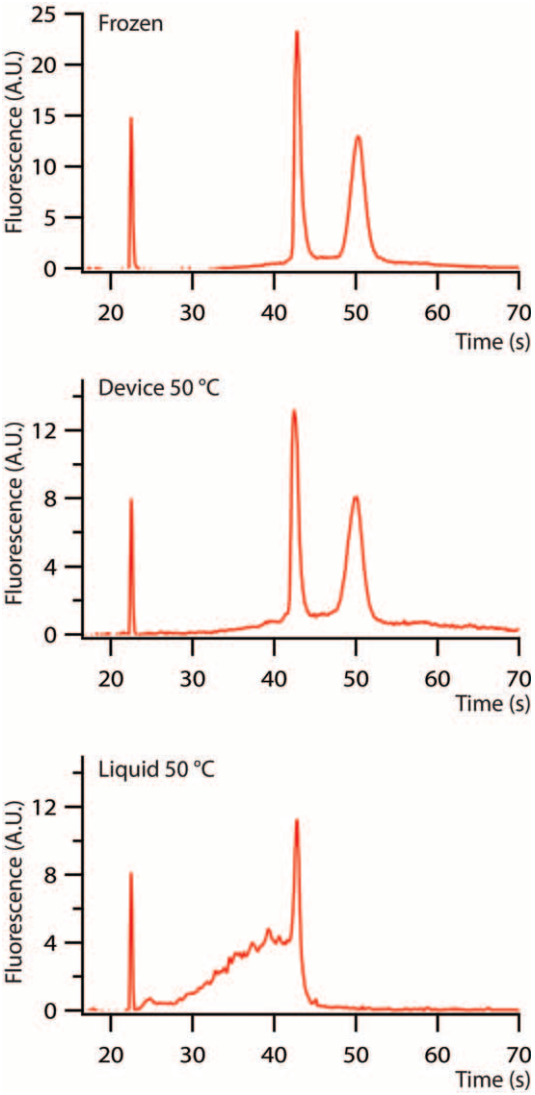

Fig. S11 Graphs showing electrophoresis results obtained with a bioanalyzer (Agilent 2100) using aliquots of control RNA (80 ng/µL) mixed with a stabilization matrix (RNAStable, Biomatrica) and stored for four days under different conditions. The first graph (top) shows the result for an aliquot of RNA stored in the traditional way (Frozen at -80 °C). The second graph (center) shows the profile for an aliquot stored dry in the described device at 50 ºC. The third graph (bottom) shows the profile for an aliquot stored in the liquid state at 50 ºC. The first two graphs show comparable profiles. The profile gives an indication of the composition of the sample, showing the size distribution of the RNA molecules.

Table S5. RNA stability evaluated using an Agilent 2100 Bioanalyzer.

Electrophoresis data show degradation of the RNA stored in the liquid state, proven by the presence of a smear of short products.

We used a semi-quantitative approach to estimate the stability of the RNA stored at different conditions. For this approach, we measured the height of the two main peaks (at 42 and 50 seconds) in Fig. S11, and calculated the ratio of those values. If there is no variation in the size distribution, we expect that the ratio of these two peaks will remain constant, no matter the global RNA concentration.

Results are the following (n=3 for each condition):

Samples	Intensity Peak 1	Intensity Peak 2	Ratio		Average	St. Dev.	95% CI
Frozen	12.2	23.1	0.53				
	13.7	26.3	0.52		**0.53**	**0.01**	**0.03**
	14.3	26.4	0.54				
Device 50°C	8	15.5	0.52				
	8.4	18.3	0.46		**0.50**	**0.04**	**0.12**
	11.7	21.7	0.54				
Liquid 50°C	0	11.7	0				
	0	17.5	0		**0**	**0**	**0**
	0	14.6	0				

The value is comparable for aliquots stored frozen and in the device (confidence intervals overlap), while the value could not be calculated for the sample stored in the liquid state, as one of the peaks was not present.

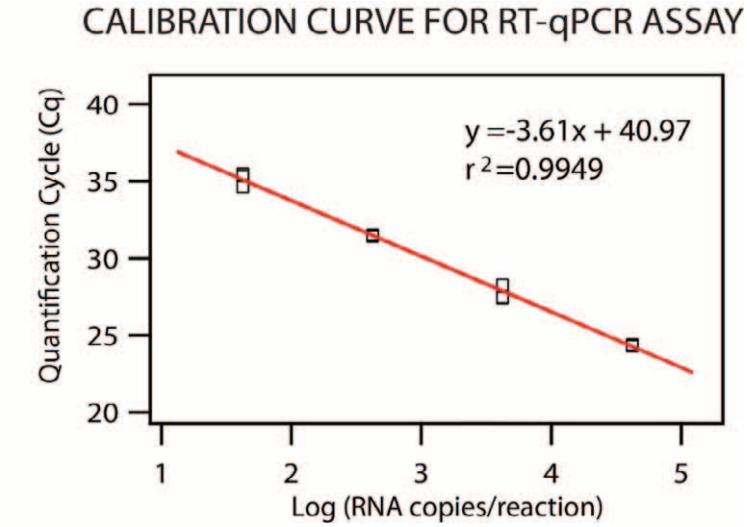

Fig. S12 Calibration curve for the RT-qPCR assay used to evaluate RNA concentration and recovery. Cq values used for calibration were reported in Table S6.
Calculated efficiency for this PCR reaction is 89%. This value was used to evaluate the recovery efficiencies in Table S4.

Table S6. Data for calibration curve shown in Figure S12.

Number of copies per RT-qPCR reactions	Log (copy number)	Cq	Average Cq	St. Dev.
42180	4.63	24.28	24.4	0.07
		24.40		
		24.40		
4218	3.63	27.5	27.7	0.5
		27.4		
		28.25		
422	2.63	31.5	32.00	0.9
		31.4		

42	1.63	35.4	35.15	0.4
		35.5		
		34.6		

Table S7. Statistical analysis for RNA storage experiments.

Statistical analysis for RNA storage experiments.
Values at different time points (n=3 for each condition)

	Frozen			Device, 50 °C			Liquid, 50 °C		
Time (days)	Cq	St. Dev.	95% CI	Cq	St. Dev.	95% CI	Cq	St. Dev.	95% CI
7	32.22	0.23	0.47	32.14	0.17	0.35	34.79	1.06	2.17
14	31.96	0.53	1.09	32.52	0.17	0.36	35.77	0.64	1.31
21	32.03	0.82	1.69	32.68	0.26	0.54	36.13	0.19	0.39
24	31.63	0.69	1.42	32.33	0.40	0.82	37.82	0.51	1.05
28	31.62	0.21	0.43	32.40	0.18	0.36	37.70	0.78	1.61
35	31.49	0.07	0.15	32.39	0.21	0.44	37.39	0.07	0.15

	Device, 25 °C			Liquid, 25 °C		
Time (days)	Cq	St. Dev.	95% CI	Cq	St. Dev.	95% CI
7	32.66	0.28	0.58	32.62	0.34	0.71
14	32.41	0.30	0.62	32.22	0.15	0.30
21	31.64	0.58	1.19	32.04	1.03	2.13
24	31.42	0.68	1.40	31.76	0.14	0.29
28	30.87	0.88	1.81	32.30	0.36	0.73
35	31.28	0.98	2.02	32.01	0.23	0.47

P-values for t-test comparing different samples
(Student T test, 2 tails, unequal variances).

Time (days)	p-value Frozen and Liquid at 50 °C	p-value Device and Liquid at 50 °C
7	0.041	0.049
14	0.0095	0.01
21	0.016	0.00024
24	0.00046	0.00020
28	0.0034	0.0048
35	6.12 E-08	0.00016

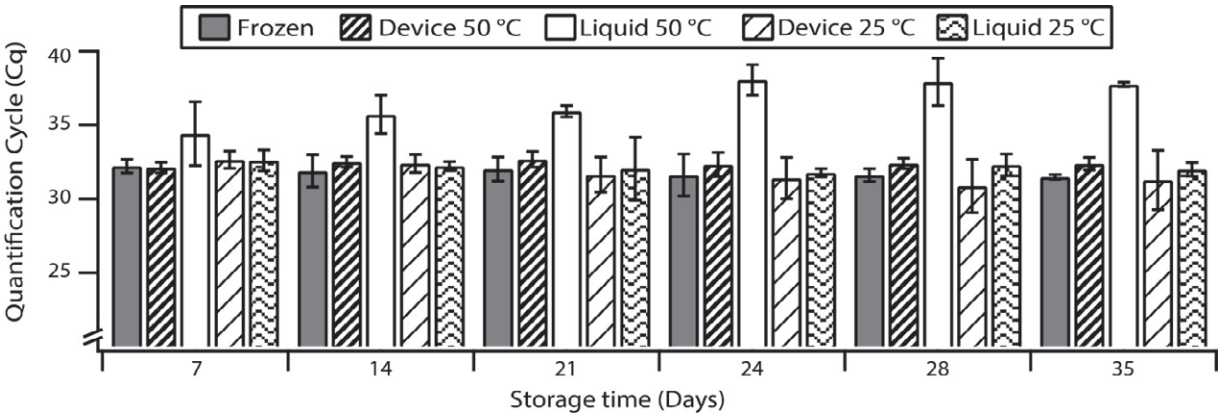

Fig. S13 A graph showing the results of quantitative analysis performed with RT-qPCR of purified HIV-1 samples all mixed with stabilization matrix. Error bars represent the 95% confidence interval (n = 3). This graph reports also data for room temperature storage, which did not show significant degradation in the presence of the stabilization matrix in the time monitored (35 days).